Life Cycle Analysis of Adaptive Building Integrated Photovoltaics

P. Jayathissa [☆a,**], M. Jansen[☆a], N. Heeren[b], Z. Nagy[a], S. Hellweg[b], A. Schlueter [a,*]

[a] *Architecture and Building Systems, Institute of Technology in Architecture, ETH Zurich, Switzerland*
[b] *Ecological System Design, Institute of Environmental Engineering, ETH Zurich, Switzerland*

Abstract

Text

Keywords: Adaptive, Solar Facade, Life Cycle Analysis, Multi Functional Envelope, BIPV

1. Introduction

Buildings are at the heart of society and currently account for 32% of global final energy consumption and 19% of energy related greenhouse gas emissions [1]. Nevertheless the building sector has a 50-90% emission reduction potential using existing technologies, and widespread implementation could see energy use in buildings stabalise or even fall by 2050. Within this strategy, building integrated photovoltaics (BIPV) has the potential of providing a substantial segment of a buildings energy needs [2]. Even the photovoltaic (PV) industry has identified BIPV as one of the four key factors for the future success of PV [3].

[☆] This document is a collaborative effort.
[*] Corresponding author
[**] Principal corresponding author
Email addresses: jayathissa@arch.ethz.ch (P. Jayathissa [☆]), heeren@ifu.baug.ethz.ch (N. Heeren), schlueter@arch.ethz.ch (A. Schlueter)

The PV industry is currently dominated by crystaline silicon photovoltaic cells due to their high efficiency and low processing costs [4]. However these technologies are often demoted as pre frabricated eco-spoilers that ruin the architectural integrity of a building [5]. This combined with their intrinsic weight restricts their large scale implementation to roofs where they are out of sight. In the last decade however, we have seen an interesting development of second generation thin film technologies [6]. In particular, $Cu(In,Ga)Se_2$ (CIGS) which is reaching competitive levels of efficiencies [7], and manufacturing costs [8] [9].

This development has brought new BIPV design possibilities. Their light weight nature and customisable shapes allows for easier and more aesthetically pleasing integration into the building envelope. Furthermore, this technology can be easily actuated and used as an adaptive building envelope [10].

Adaptive buildings envelopes have gained interest in recent years due to their energy saving potentials [11]. From an energetic perspective, the envelope acts as a buffer between the interior and exterior environments. An adaptive building envelope can mediate solar isolation on the building, thereby offering reductions in heating/cooling loads and improvement of daylight distribution [10]. Interestingly the mechanics that actuate adaptive envelopes couples seamlessly with the mechanics required for facade integrated PV solar tracking. The balance of electricity production, and adaptive shading can in some cases offset the entire energy demand of an office space behind this adaptive envelope [12]. We call this combination of technologies an Adaptive Solar Facade (ASF).

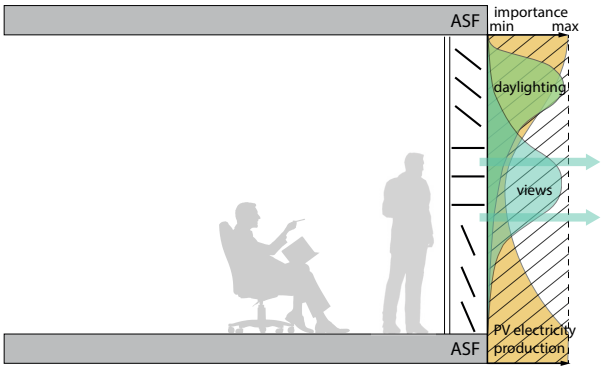

Figure 1: The facade acting as a mediator between the interior and exterior environment, while fullfilling various functions [13]

The design of an ASF comes at an added cost. The additional electronics, actuators, and supporting structure adds further embodied CO2 to the Balance of Systems (BOS). In this paper we will discuss the ASF from a life cycle perspective thus analysing whether the increase in operational savings offsets the increased embodied carbon.
The remainder of the paper is organised as follows. In the next section we describe the inventory of an ASF, the operational emissions and LCA methadology used in this analysis. In Section 3 we will present the results from the LCA and look at the major sources of embodied carbon, along with the operational performance. In this section we will also compare the results of the LCA with other technologies and the effects in different regions. In Section 4 we discuss the results and possible implications this will have on the future design of Adaptive Solar Facades.

2. Methodology

The analysis looks at the embodied carbon in production, operation, and disposal of the Adaptive Solar Facade (ASF).

2.1. Embodied Energy Inventory and Assumptions

The ASF is composed of six sub-product systems described in Figure 2. This consists of CIGS PV panels mounted on an actuator, supported by a cantilever that offsets it from a cable net supporting structure. An exploded view of these components can be seen in Figure 3.

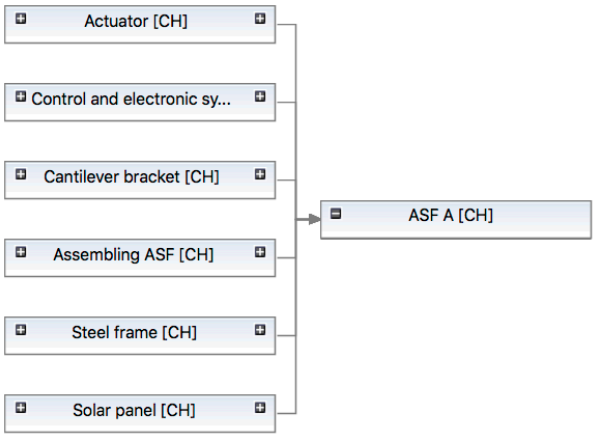

Figure 2: Breakdown of the ASF into six sub-product systems (Note change Steel frame to Suporting Structure, and Assembling ASF to Assembly. Also redraw this chart so it matches the subsubsections below)

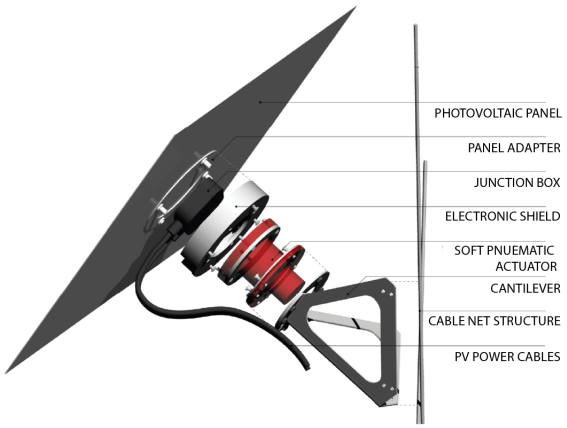

Figure 3: Exploded view of an ASF module mounted on a cable net supporting structure

PV Panel

The PV panels that can be used are restricted by their weight. Therefore, any technology that requires glass encapsulation or a heavy substructure cannot be used. This limits us to CIGS and amorphous silicon panels [Check

this fact again]

CIGS PV panels was selected as the thin film panel of choice due to its high efficiency, low cost, and ability to be deposited on a polymer or aluminium substrate [14]. A less efficient thin film amorphous silicon panel could also be used and will also be discussed in this analysis.

Panel Type	Embodied Carbon	Efficiency
CIGS	XXg/m2	YY%
a-Si	YY g/m2	YY%

Table 1: Possible PV technologies for an ASF [Ref required]

CIGS	xx g/m2
Junction Box	
Power Cables	

Table 2: Inventory of main input flows to the PV manufacturing process [ref required]

Actuator

Traditionally photovoltaic actuation is done through the use of servo motors. Servo motors however become a limiting factor for adaptive facades due to their high upfront costs, and instability in heavy winds. Soft robotic actuators on the other hand are cheaper and more resilient to harsh environmental conditions[15]. For the purpose of this analysis we will analyse both servo motors and soft robotic actuators.

Compressor	xxg/unit
Tubes	xxgCO2/m
Silicone	xxgCO2/yy

Table 3: Inventory of main input flows to the Actuator manufacturing process [ref required]

Cantilever

The cantilever is a steel connection point between the PV panel and the supporting structure.

Steel	xxgCO2/yy
xxxx	xxgCO2/yy
yyyyy	xxgCO2/yy

Table 4: Inventory of main input flows to the Cantilever manufacturing process [ref required]

Supporting Structure

The supporting structure is the connection point between the array of photovoltaic modules and the building itself. Many different designs are possible, however we will base our analysis of an adaptive solar facade that has already been constructed [13]. This design consists of a steel cable-net that spans a steel supporting frame. The steel frame is then attached to the building itself.

Steel	xxgCO2/yy
xxxx	xxgCO2/yy
yyyyy	xxgCO2/yy

Table 5: Inventory of main input flows to the manufacturing process of the Supporting Structure[ref required]

Controls and Electronic System

The control system is required for the actuation of panels and the regulation of photovoltaic electricity production.

Steel	xxgCO2/yy
xxxx	xxgCO2/yy
yyyyy	xxgCO2/yy

Table 6: Inventory of main input flows to the manufacturing process of the Control System[ref required]

Installation

The installation of the ASF to the building requires a hydraulic hoist which needs to be in operation for eight hours based off previous construction experience [12].

Steel	xxgCO2/yy
xxxx	xxgCO2/yy
yyyyy	xxgCO2/yy

Table 7: Inventory of main input flows to the Assembly Process[ref required]

2.2. Operational Emissions and Assumptions

The potential savings are based off previously completed numerical simulations [12]. The simulation was conducted on a south facing office room. The room xx meters in length, xx meters wide and xx meters high was modeled using Rhinoceros 3D CAD Package [16], shown in Figure XX. Grasshopper [17] was used to model the dynamic aspects of the ASF which consists of an array of 400mm CIGS solar panels. The geometrical input is imported to Energy Plus [18] though the DIVA [19] interface. A single zone thermal analysis was conducted for each possible geometrical configuration of the ASF for each hour of the year. The results were then post processed in Python [20] with the NumPy [21], and pandas [22] plug-ins.

Based on the assumption of XX full openings and closings per day, we approximate the energy requirement to actuate the ASF to be YY kWh in its lifetime.

Building Settings	
Office Envelope	Roof: Adiabatic Floor: Adiabatic Walls: Adiabatic Window: Double Glazed LoE (e=0.2) 3mm/13mm air Floor Area: 21.7m2
Thermal Set Points	Heating: 22 degrees Celcius Cooling: 26 degrees Celcius
Lighting Control	Lighting set point: 11.8W/m2 Lighting Control: 300 Lux Threshhold
Occupancy	Office: Weekdays from 8:00-18:00 People set point: 0.1 persons/m2 Infiltration: 0.5 per hour
Location Assumptions	
Weather File	Geneva, Switzerland
Electricity Mix	UCTE
Maintenance	
xxxx	xxxx
ASF Settings	
Full open and closes per day	yy

Table 8: Summary of main assumptions for the calculation of operational emissions [ref required]

2.3. Evaluation Method (Under heavy Construction)

- The analysis is performed according to ISO 14040, ISO 14044 and ISO 15804.
- The impact category, which will be evaluated, is the global warming potential (GWP). This is described as the emissions of $CO_2 - \text{eq}$ in kilograms divided by the functional unit.
- The functional unit used is twofold and based on the function of the adaptive building envelope. For the comparison with other shading systems facade area in m^2 is used, while comparison with other photovoltaic systems is done using electricity produced in kWh. According

to the guidelines of the International Energy Agency (IEA), the calculation of kWh produced needs to be based for consistency on conversion efficiency η, performance ratio PR, irradiation I, lifetime LT and area A of the module. Equation 1 gives the exact formulation:

$$G = \frac{\text{GWP}}{\text{I} \cdot \eta \cdot \text{PR} \cdot \text{LT} \cdot \text{A}} \tag{1}$$

- The LCI inventory was obtained through...
- The scope of the LCA comprises the embodied, operational and disposal global warming impact of the respective system. Figure 4 illustrates the system boundaries of the process flows. The supporting structures are also included in the system boundaries. The reason for this is that technologies within the building envelope also change the design of the supporting structures. The supporting structure of solar panels is referred to as balance of systems (BOS).

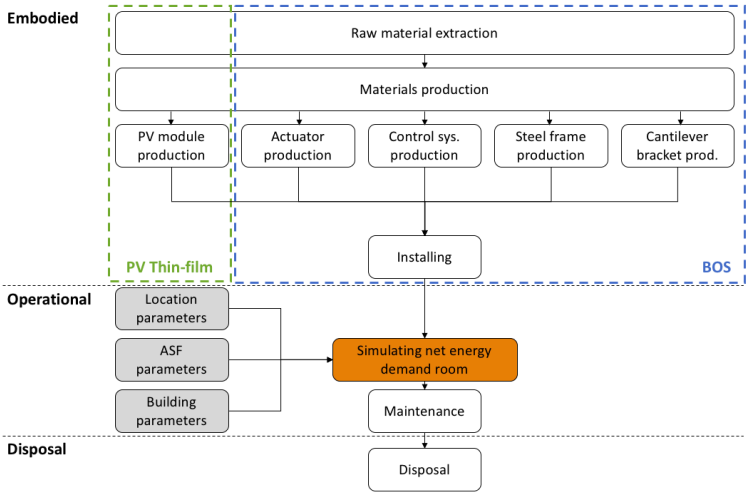

Figure 4: Thin-film incl. BOS system boundaries

- The cut-off approach is used for recycling and landfill. This means that recycling does not generate any credit for the product and resulting benefits are not taken into account. Furthermore the use of recycled products do not bear the burden of processes higher up the chain.

- The recipe midpoint (H) allocation method allows for an accurate evaluation of the GWP based on human impact factors.

3. Results

3.1. LCA of the Adaptive Solar Facade

A breakdown of the embodied carbon emissions can be found in Figure 5. It can be seen that the largest emboodied global warming potential (GWP) contribution in the ASF comes from the solar panels, the electronics and the steel frame.

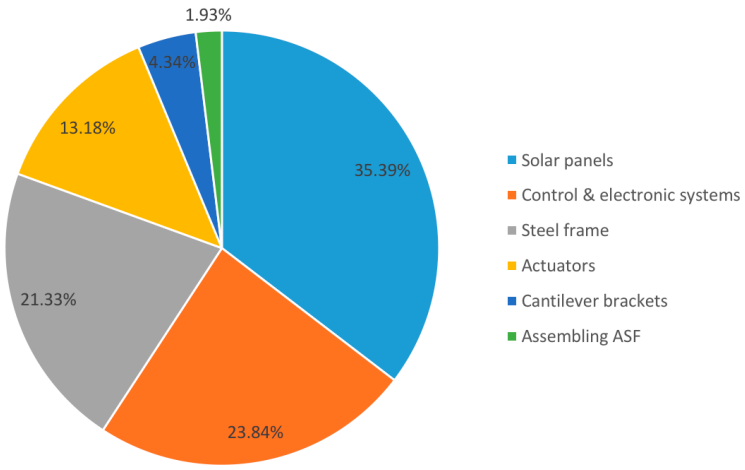

Figure 5: Breakdown of the embodied carbon emissions, it can be seen that xxxx has the greatest GWP contribution

It is interesting to note that the choice of actuation system for an ASF can have a significant / minimal impact on the embodied emissions. [Elaborate further when results come in]

The operational energy consumption of the office space behind the ASF was compared to a case with a static louvered based shading system at 45° and a case with no shading at all. We calculated a total energy saving of 25% compared to louvers at 45° and 56% compared to a case with no facade shading [12]. These results are sumarised in Figure 6. Note that this figure does not include on site electricity generation.

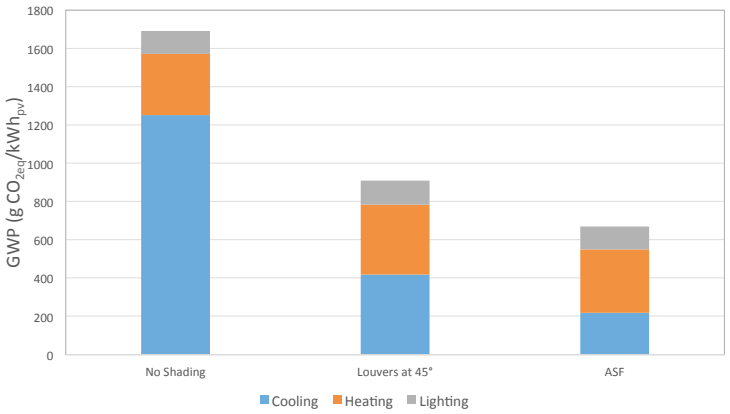

Figure 6: Breakdown of the opperational carbon emissions, we can see a added savings of 24% compared to a static louvered shading system and 56% compared to no shading system at all

The total GWP of the ASF can be built up using a waterfall chart, Figure 7. To calculate the emission factor (gCO_2eq/kWh) we subtract the total embodied energy by the savings through our shading algorithm. We then add the GWP values for maintenance and disposal to achieve a total GWP over the 20 year life time of the ASF. This total is then used to calculate the emission factor of electricity produced by the ASF ($126.8gCO_2/kWh$).

It can be seen that the embodied GWP of the ASF is greater than a classical PV installation, however most of that initial investment is offset through the reduction of heating, cooling and lighting loads. Maintenance and disposal takes up roughly 10% of all total carbon emissions.

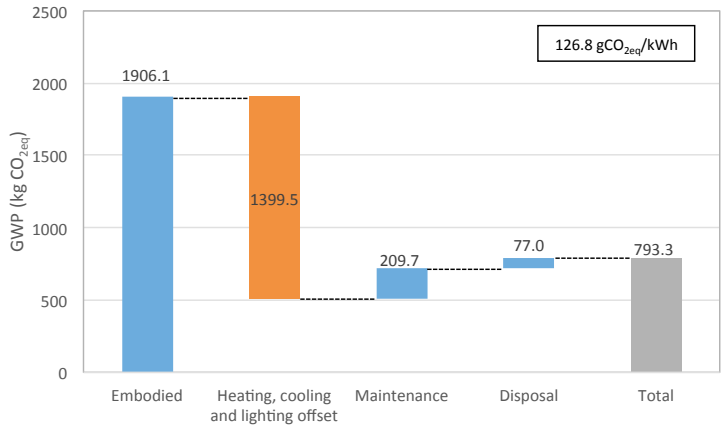

Figure 7: Waterfall diagram of GWP of the ASF. The far left column details the embodied carbon emissions. The second bar details the emission reduction of the building through the smart shading algorithms of the ASF. The third column shows an increase of emissions through maintenance. The fourth column shows an increase in emissions in the disposal. This leaves us with a final emissions value. When we apply this value to Equation 1 we obtain an emission factor per kwH of 126.8gCO_2/kWh.

3.2. Global Distribution of GWP and Terrestrial Acidification

The global distribution of embodied GWP emissions is focused in Europe, specifically Germany and Switzerland as most of the manufacturing is done in this region. It can be see however that emissions occur globally due the sourcing of primary materials from many locations around the world. Terrestrial acidification however is more interesting as it has a local impact compared to carbon emissions. It is interesting to note that China carries the greatest burden of terrestrial acidification from the ASF production.

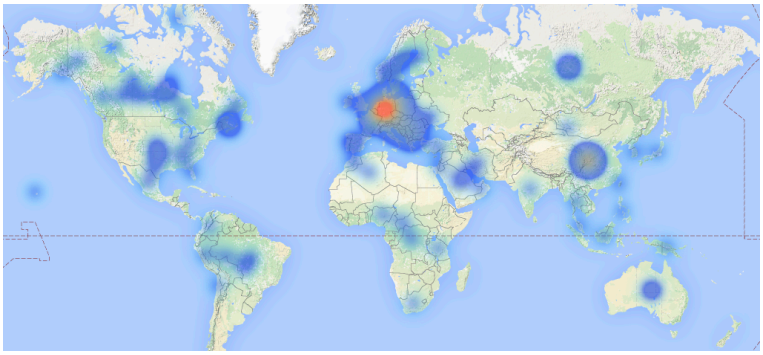

Figure 8: Global distribution of embodied GWP emissions

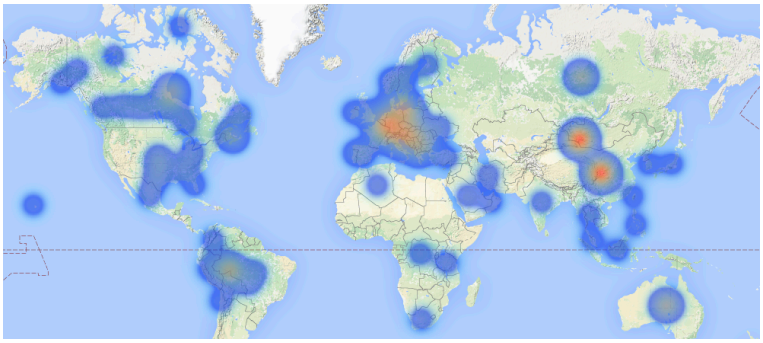

Figure 9: Global distribution of terrestrial acidification

3.3. Sensitivity Analysis

Changing the assumptions can have a significant impact on the LCA result. Three assumptions were evaluated in the sensitivity analysis: Operation location, type of PV panels, and the type of actuation system. The inputs are summarised in Table 9 with the results shown in Figure 10.

It can be seen that the operation location has a significant impact on the carbon saving potential. In Switzerland, we see a 6% reduction compared to the average electricity mix. This is because the Swiss electricity mix is dominated by hydro and nuclear which has a very low GWP potential [citation needed]. In Germany on the other hand, the ASF has a 81% reduction in carbon emissions as the emission factor of the electricity grid is roughly five

Assumption	Case A	Case B
Operation Location	Switzerland	Germany
PV Panel type	a-Si	CIGS
Actuator Type	Servo Motor	Soft Robotic Actuator

Table 9: Inputs to the Sensitivity Analysis Conducted

times higher compared to Switzerland [citation needed]. The actuators and Pv panel type had a ...

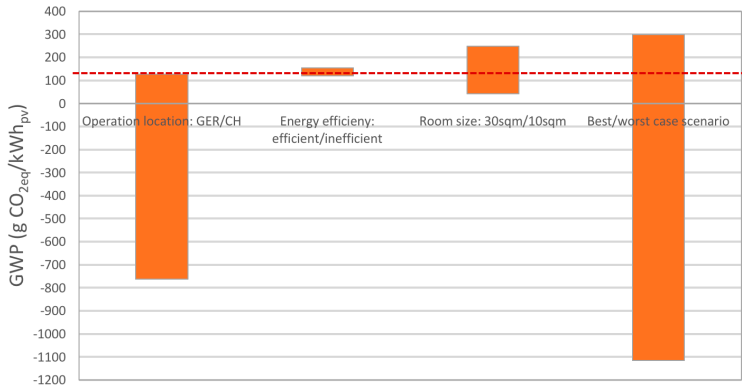

Figure 10: Sensitivity analysis of the emission factor based on location of use, panel type, and actuator type (Wrong Figure)

3.4. Comparison to existing PV technologies

Comparison of the ASF to other PV technologies and the UCTE electricity mix is highlighted in Figure 11. We can see in this figure that the ASF without shading benefits is inferior to all other technologies. It is only with the added shading benefits that we really see the advantages of the adaptive system. We can also see that the utilisation of the ASF in an area where the electricity mix has low GWP intensity such as Switzerland also has disadvantages. It is capable of out performing Silicone based technologies but is still inferior to simply mounted CIGS panels. Note that even the panels themselves of the ASF, without the BOS, is still lower that the CIGS installation. This is due to the added inefficiencies as the panels are not always at the optimum position to the sun.

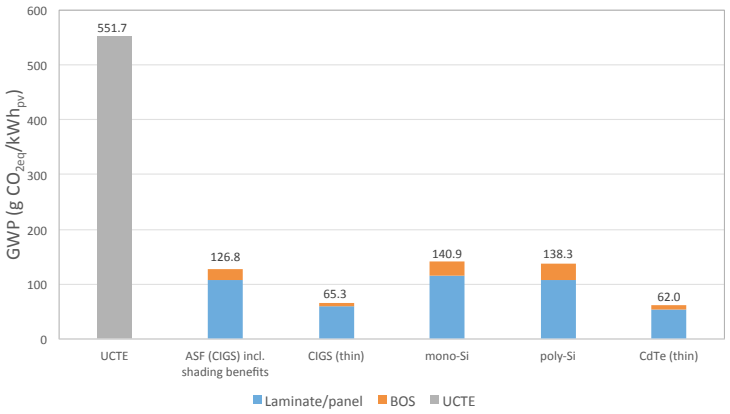

Figure 11: Comparison of thin-film and BOS to other PV technologies. I would add some extra columns, one without shading, one with the ASF in Switzerland, one with the ASF in Europe

4. Discussion

- When is the ASF advantages, when is it not
- Would it be better to just have a optimally angled static system?
- Limitations of the study
- Nuclear power in France and Switzerland
- No need to purchase land, advantage of facade integration
- What should designers of adaptive solar facades keep in mind
- Other advantages of the ASF that are not clear in the LCA analysis, such as daylighting and user centered control
- Have a technology where you can put PV where you normally can't put PV

5. Conclusion

- xxx% of Embodied emissions of the photovoltaic BOS can be offset through smart shading
- This multi functionality brings about new advantages/disadvantages for solar as it has a reduced/increased the emissions per kWh by xxx%
- Higher embodied CO2 compared to a classic photovltaic retrofit. However reduction can be made through x y and z
- Results are highly sensitive to x y and z

- Have a technology where you can put PV where you normally can't put PV

6. Acknowledgments

...

References

[1] Fifth assessment report, mitigation of cliamte change, Intergovernmental Panel on Climate Change 674–738.

[2] S. T. et al., 14th Euro Conf. Photovoltaic Solar Energy Conversion.

[3] M. Raugei, P. Frankl, Life cycle impacts and costs of photovoltaic systems: current state of the art and future outlooks, Energy 34 (3) (2009) 392–399.

[4] T. Saga, Advances in crystalline silicon solar cell technology for industrial mass production, npg asia materials 2 (3) (2010) 96–102.

[5] C. Lueling, Energising Architecture, Jovis, 2009.

[6] G. Wilson, NREL cell efficiency records, National Center for Photovoltaics.

[7] K. Kushiya, Cis-based thin-film pv technology in solar frontier kk, Solar Energy Materials and Solar Cells 122 (2014) 309–313.

[8] M. Kaelin, D. Rudmann, A. Tiwari, Low cost processing of cigs thin film solar cells, Solar Energy 77 (6) (2004) 749–756.

[9] B. P. Jelle, C. Breivik, H. D. Røkenes, Building integrated photovoltaic products: A state-of-the-art review and future research opportunities, Solar Energy Materials and Solar Cells 100 (2012) 69–96.

[10] D. Rossi, Z. Nagy, A. Schlueter, Adaptive distributed robotics for environmental performance, occupant comfort and architectural expression, International Journal of Architectural Computing 10 (3) (2012) 341–360.

[11] R. Loonen, M. Trčka, D. Cóstola, J. Hensen, Climate adaptive building shells: State-of-the-art and future challenges, Renewable and Sustainable Energy Reviews 25 (2013) 483–493.

[12] P. Jayathissa, Z. Nagy, N. Offedu, A. Schlueter, Numerical simulation of energy performance and construction of the adaptive solar facade, Advanced Building Skins, TU Graz 2.

[13] Z. Nagy, S. Bratislav, J. Prageeth, B. Moritz, H. Johannes, L. Gearoid, W. Anja, A. Schlueter, The adaptive solar facade: From concept to prototypes, under review.

[14] A. Chirilă, S. Buecheler, F. Pianezzi, P. Bloesch, C. Gretener, A. R. Uhl, C. Fella, L. Kranz, J. Perrenoud, S. Seyrling, et al., Highly efficient cu (in, ga) se2 solar cells grown on flexible polymer films, Nature materials 10 (11) (2011) 857–861.

[15] B. Svetozarevic, Z. Nagy, D. Rossi, A. Schlueter, Experimental Characterization of a 2-DOF Soft Robotic Platform for Architectural Applications, Robotics: Science and Systems, Workshop on Advances on Soft Robotics (2014) 2–6.

[16] Rhinoceros v5 (2015).
URL `https://www.rhino3d.com/`

[17] Grasshopper - algorithmic modeling for rhino (2015).
URL `http://www.grasshopper3d.com/`

[18] B. T. Office, Energy plus.
URL `http://apps1.eere.energy.gov/buildings/energyplus/`

[19] Diva for rhino.
URL `http://diva4rhino.com/`

[20] Python.
URL `https://www.python.org/`

[21] Numpy.
URL `http://www.numpy.org/`

[22] pandas.
URL `http://pandas.pydata.org/`